

Received February 1, 2019, accepted February 24, 2019, date of publication March 1, 2019, date of current version March 20, 2019.

Digital Object Identifier 10.1109/ACCESS.2019.2902460

# Design and Analysis of a Novel Synthetic Slot Dual-PM Machine

XINHUA GUO<sup>1</sup>, QIUXUE WANG<sup>1</sup>, RONGYAN SHANG<sup>1</sup>, FENYU CHEN<sup>1</sup>,  
WEINONG FU<sup>2</sup>, AND WEI HUA<sup>3</sup>, (Senior Member, IEEE)

<sup>1</sup>College of Information Science and Engineering, Huaqiao University, Xiamen 361021, China

<sup>2</sup>Department of Electrical Engineering, The Hong Kong Polytechnic University, Hong Kong 999077

<sup>3</sup>School of Electrical Engineering, Southeast University, Nanjing 210096, China

Corresponding author: Wei Hua (huawei1978@seu.edu.cn)

This work was supported in part by the National Natural Science Foundation of China under Project 51477058 and Project 51707068, in part by the Science and Technology Planning Project of Fujian Province under Project 2017H0021, in part by the Promotion Program for Young and Middle-aged Teacher in Science and Technology Research of Huaqiao University under Project ZNQ-YX304, and in part by the Opening Foundation of the Key Laboratory of Power Electronic Drive, Chinese Academy.

**ABSTRACT** We propose a novel synthetic slot dual-permanent-magnet (SSDPM) machine with high-torque density for direct drive in-wheel electric vehicles that employ two sets of permanent-magnet (PM) motors. The SSDPM uses both PMs on the rotor and the stator slots, which can achieve flux modulation. The machine's operating principles, based on bidirectional flux modulating effects, need to be further developed. In SSDPM stator slots, PMs are located on the rabbet and on each side of a tooth. The PM is magnetized in various ways and its arrangement is more flexible. A magnet-iron structure is used to provide the flux modulation and PM excitation concurrently. The optimal design adopts a combined method that uses a finite element method and a genetic algorithm. The performance of this hybrid method is analyzed by simulation. A prototype machine is manufactured and the experimental results verify the validity of the model structure and simulation results.

**INDEX TERMS** Flux modulation, genetic algorithm (GA), magnet-iron structure, synthetic slot.

## I. INTRODUCTION

Electric vehicles (EV) have long been considered as one of the most effective solutions to mitigate the urgent energy, pollution, global warming and environmental challenges facing our society [1]–[5]. To achieve high performance, mechanical gears are arranged to match their wheels. However, mechanical gears have attracted little attention (which is possibly) due to mechanical vibration, frictional losses, regular lubrication and maintenance [6], [7]. By individual control, simple transmission mechanisms and high efficiency can be achieved via in-wheel motors.

Recently, a new set of magnetic gear-based machines (MGMs), with an operation principle is based on the modulation of magnetic fields, have been proposed [8]–[11]. To enhance torque density, MGMs and in-wheel direct-drive motors are combined [12]. Nevertheless, the torque transmission capability of this combination is still low. To improve machine's torque density, hybrid-excited machines with both PM and coil current excitations have

been proposed [13]–[15]. However, the PMs are located on the rotor or stator. Therefore, the limit of PM materials will influence the machine's performance. For the purpose of improving the torque density, dual-rotor PM machines have been designed and verified [16]–[18]. However, the poor heat dissipation capacity in a region surrounding dual-rotor PMs may cause irreversible demagnetization. To address this challenge, and further improve torque density, dual-stator PM machines are proposed [19], [20]. The double stator-PM structure can improve the machine's utilization ratio and help to cool the magnets. However, there are some limitations to dual-stator PM topologies, e.g., PM use is still constrained.

The purpose of this paper is to propose a novel machine that has two sets of PMs located on the rotor and stator. Both the fundamental components produced by PMs and harmonics produced by the flux modulation can contribute to improving the torque density. Meanwhile, a new synthetic slot structure is proposed that can fully utilize the inner space of stator slots. Moreover, the PM locations are flexible, different topologies of synthetic slots dual-PM (SSDPM) machine can be developed. The performance of the proposed machine is via 2D finite element method (FEM) and genetic

The associate editor coordinating the review of this manuscript and approving it for publication was Mustafa Servet Kiran.

algorithm (GA), and experimentally verified by a prototyped machine [21].

## II. DESIGN

Fig. 1 shows the topology of a SSDPM machine for the direct-drive in-wheel system in EVs. The machine consists of two rotors and double stator. In one of the synthetic slots, a PM is mounted on the surface, which is magnetized radially outwards. The remaining PMs are installed on the left and right side of stator outer slots, and magnetized along with clockwise and counterclockwise directions, respectively.

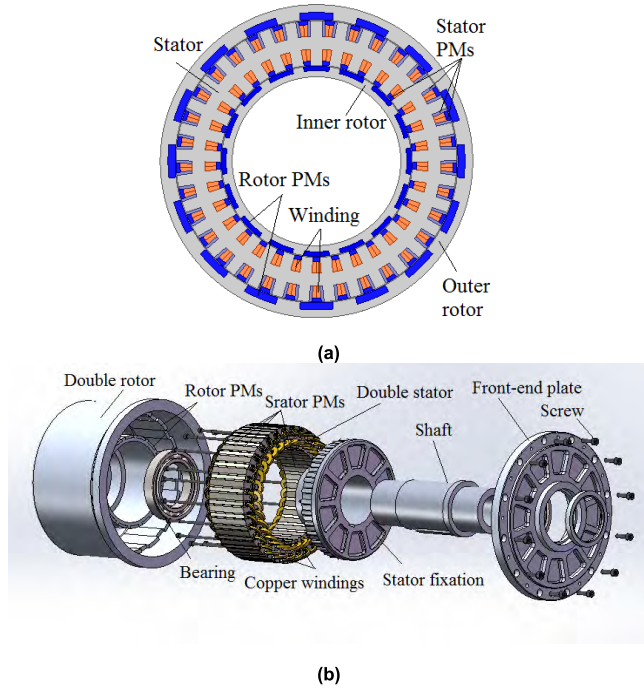


**FIGURE 1.** The topology of the proposed SSDPM machine. (a) 2D topology. (b) 3D topology.

### A. BASIC DESIGN RULES

For dual-PM machines, the operating principle is based on the flux modulating effect. In that case, the two sets of PMs should employ magnet-iron structure. In addition to the fundamental components excited by the poles of PM, various field harmonics can be induced by any uneven magnetic field paths [22], [23]. Then, the same PPN and rotating speeds of the harmonics can couple together to generate a steady electromagnetic torque. To reveal the working principle of the proposed machine clearly, the harmonics excited by the PMs and armature currents are analyzed.

The magnetic field excited by the stator PMs are considered next. The rotor's iron teeth will interact with the magnetic field generated by the stator PMs and additional field harmonic components can be produced. Therefore, the PPN and rotational speed can be expressed as

$$\begin{cases} p_{(m,n)}^s = (mp_s + np_r) \\ \Omega_{(m,n)}^s = \frac{np_r}{mp_s + np_r} \Omega_r \end{cases} \quad (1)$$

**TABLE 1.** Effective field harmonics.

Group	Combination	Pole-pair number	Rotation speed
Group 1	$m=1, n=0$	$p_w$	$\Omega_w$
Group 1	$m=1, n=0$	$p_w$	$\Omega_w$
Group 1	$m=1, n=-1$	$p_w$	$-p_r \Omega_r / p_w$
Group 1	$m=1, n=-1$	$p_w$	$-p_r \Omega_r / p_w$
Group 2	$m=1, n=-1$	$p_r$	$-p_w \Omega_w / p_r$
Group 2	$m=1, n=0$	$p_r$	$\Omega_r$
Group 3	$m=1, n=1$	$p_s$	$(p_w \Omega_w + p_r \Omega_r) / p_s$
Group 3	$m=1, n=0$	$p_s$	0

where  $m = 1, 2, 3, \dots, \infty$  and  $n = 0, \pm 1, \pm 2, \pm 3, \dots, \pm \infty$ . The pole-pair number of the PMs on the rotor are labelled  $p_r$ . The tooth number serves as the modulation component in the stator and is characterized by the term  $p_s$  and the rotational speed of the rotor is  $\Omega_r$ .

We evaluate the magnetic field excited by the rotor PM next. The PPN and rotational speed can be written in the following form

$$\begin{cases} p_{(m,n)}^r = (mp_r + np_s) \\ \Omega_{(m,n)}^r = \frac{mp_r}{mp_r + np_s} \Omega_r \end{cases} \quad (2)$$

We note that the magnetic fields are now excited by two sets of PMs that should interact with the armature. The PPN of the magnetic field, excited by two sets of PMs, can be written as

$$\begin{cases} p_{(m,n)}^{w,r} = (mp_w + np_r) \\ p_{(m,n)}^{w,s} = (mp_w + np_s) \end{cases} \quad (3)$$

where  $p_w$  is the number of pole-pairs of the armature winding. The rotational velocity of the harmonics excited by two sets of PMs can be expressed as

$$\begin{cases} \Omega_{(m,n)}^{w,r} = \frac{mp_w}{mp_w + np_r} \Omega_w + \frac{np_r}{mp_w + np_r} \Omega_r \\ \Omega_{(m,n)}^{w,s} = \frac{mp_w}{mp_w + np_s} \Omega_w \end{cases} \quad (4)$$

where  $\Omega_w$  is the rotational velocity of the fundamental component in the armature winding. The effective field harmonics in each group can generate stable electromechanical energy conversions. They are listed in Table 1. The rotating speed of these effective harmonics should satisfy

$$\Omega_r = -\frac{p_w}{p_r} \Omega_w \quad (5)$$

Equation (5) suggests that the PPN and rotating speed of the proposed machine can be modulated like a magnetic gear. This machine is a combination of an outer-rotor PM machine and inner-rotor PM machine. Moreover, the two machines are based on a bidirectional flux modulating effect. Once these two machines are combined into one frame, they offer higher torque capabilities than the separated flux-modulated machines.

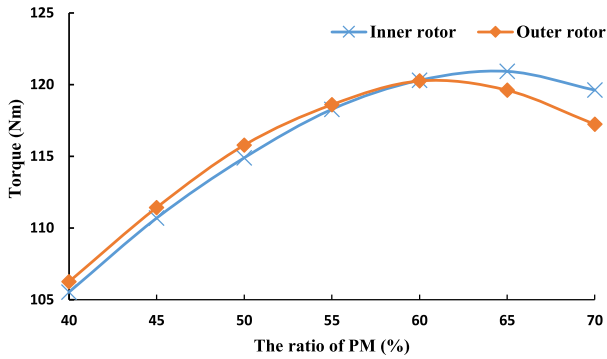


FIGURE 2. Torque variation versus PM ratio.

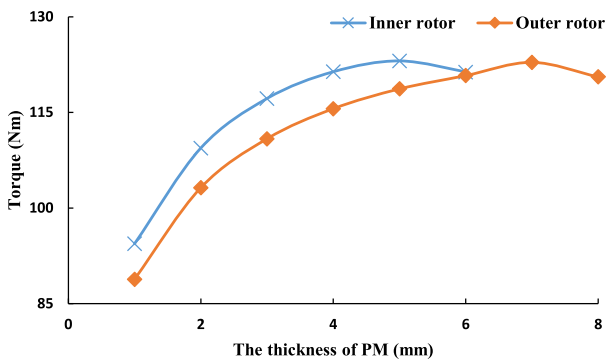


FIGURE 3. Torque variation versus PM thickness.

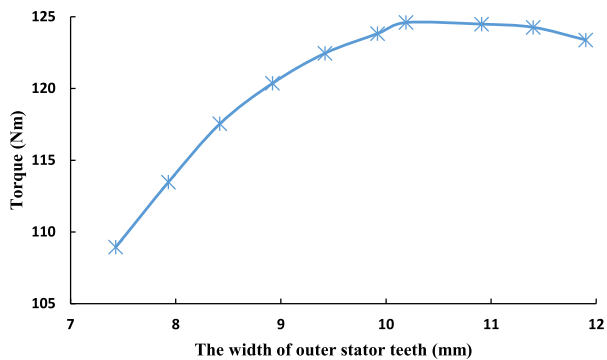


FIGURE 4. Torque variation versus stator teeth width.

**B. DESIGN OPTIMIZATION**

To investigate the influence of the geometric parameters on the torque performance of the machine, as shown in Fig. 2 and Fig. 3. The parametric analysis is measured according to the ratio and thickness of the rotor. The effect of width on the torque of the outer stator tooth is also investigated and shown in Fig. 4.

To improve the proposed machine performance, an FEM-GA coupled method is employed. The flowchart for the method is shown in Fig. 5. In this work, we use software to conduct a finite-element analysis and the GA algorithm is used to perform an optimization. To generate the next value, Visual Studio is adopted. The values generated by programming will be simulated and analyzed by calling the FEM Maxwell package. The results of the

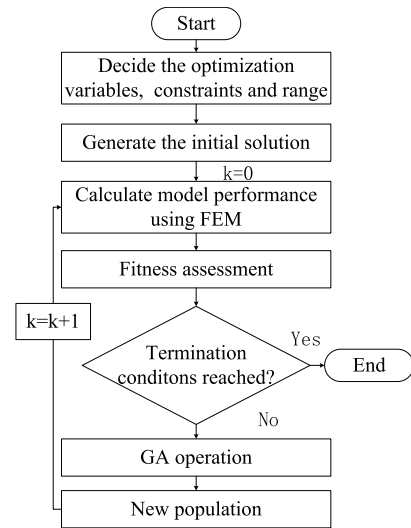


FIGURE 5. Optimal design process of the SSDPM machine.

TABLE 2. Key parameters to be optimized and corresponding limits.

Parameters	Upper value	Lower value
Inner rotor PM thickness (mm)	5	2.5
Inner rotor PM ratio	70%	35%
Stator outer tooth width (mm)	11.5	7
Outer rotor PM thickness (mm)	8.1	2.7
Outer rotor PM ratio	65%	30%

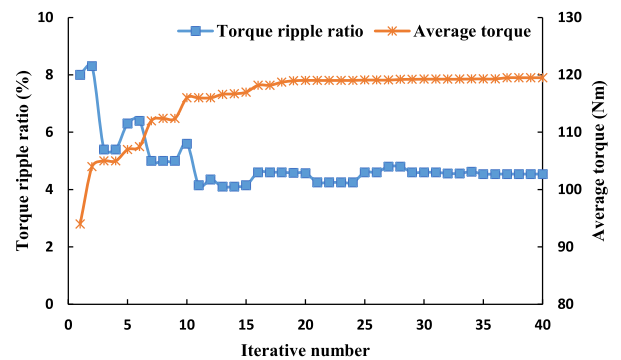


FIGURE 6. Average torque and torque ripple ratio at different iterative numbers.

simulation are then uploaded to the program software for evaluation. In addition, the proposed machine will optimize other structural dimensions via scanning parameters. In this optimization process, the outer rotor diameter, axial length, and rotor topology are kept constant. Five key parameters are set as optimization variables and listed in Table 2. The objective function determines the optimal output torque with a constraint that the torque’s ripple ratio is smaller than 10%. The population size of the genetic algorithm is 100.

Fig. 6 shows the optimization results of the iterative number and the average torque output. Correspondingly, the torque ripple ratio is within a limited range. The optimization process converges rapidly, which demonstrates the

TABLE 3. Final parameters of the SSDPM machine.

Parameters	SSDPM machine
Rotor outer diameter (mm)	240
Axial length (mm)	65
PPN of outer rotor PMs	16
PPN of armature windings	17
Number of stator slots	33
PPN of inner rotor PMs	16
Rated speed (rpm)	1000
Rated power (Kw)	12.5
Number of phase	3

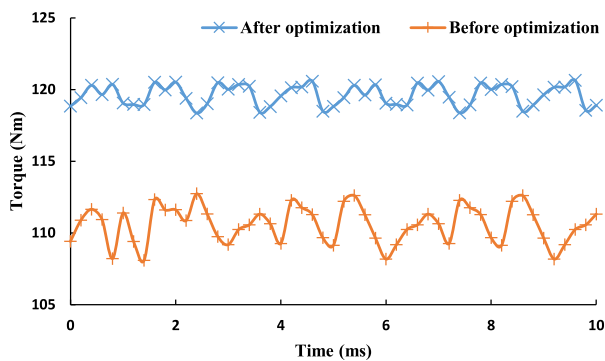


FIGURE 7. Torque capability of the proposed machine at 1000rpm.

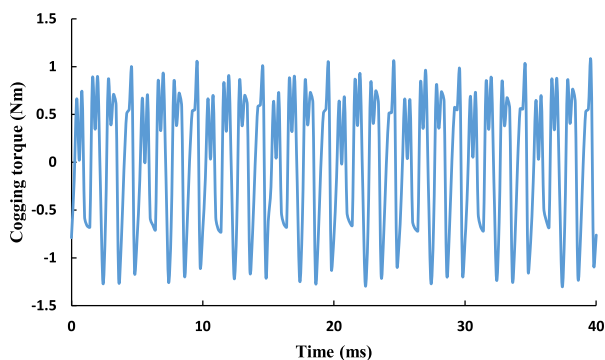


FIGURE 8. Cogging torque capability of the proposed machine at 1000rpm.

effectiveness of the coupled FEM-GA method. Finally, the optimized parameters are listed in Table 3.

### III. PERFORMANCE ANALYSIS

Fig. 7 shows the electromagnetic torque waveforms of the proposed SSDPM machine at 1000 rpm. After optimization of the structure parameters, the output torque is significantly improved. The cogging torque is small, as shown in Fig. 8.

To verify the performance of the synthetic slots, an experiment is conducted with an armature winding current of 80A and a rotor speed of 600 rpm. The torque density produced by both the stator-PMs and rotor-PMs, the rotor-PMs only, and the stator-PMs only, are compared and shown in Fig. 9. Neglecting the nonlinear effect of the magnetic paths, the proposed SSDPM machine can be viewed as a combination of

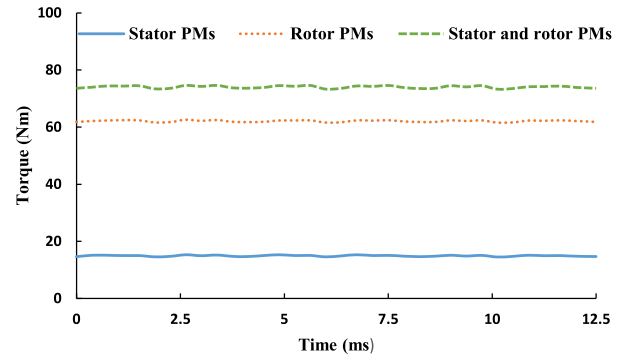
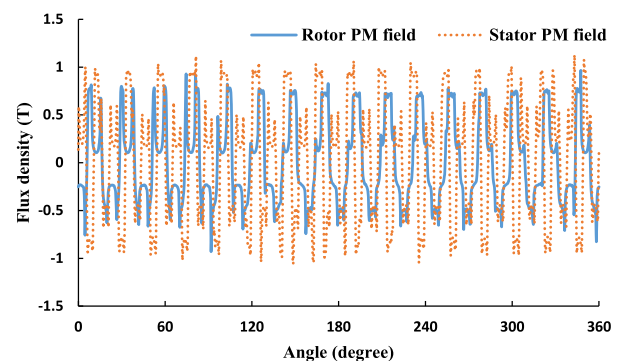
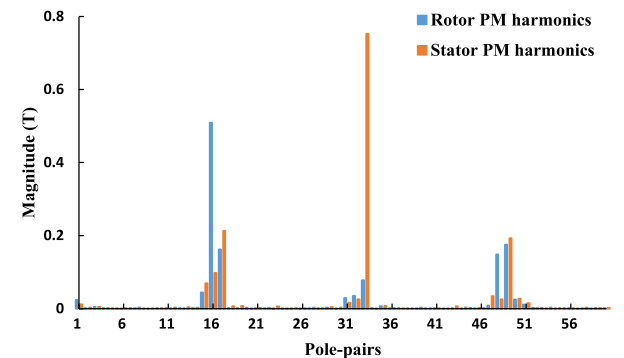


FIGURE 9. Torque capability at 600rpm.



(a)



(b)

FIGURE 10. The outer air-gap field distributions and harmonic spectrum. (a) Air-gap flux density distributions. (b) Air-gap flux density space harmonic spectra.

two separated PM machines, where one is rotor-PM-excited and the other is stator-PM-excited.

To further illuminate the basic theory, the outer air-gap field distributions and harmonic spectrum is shown in Fig. 10. The results are based on the dual-flux-modulating effect. Thus, the stator's outer slots PMs, the outer rotor steels, and the winding on the stator outer slots consist of the first flux modulation group. The stator's outer slot steels, the outer rotor PMs, and the windings on the stator's outer slots consist of the second flux modulation group. According to the field excited by the stator and rotor PMs, the main harmonics can also occur on the 16th, 17th and 33th. The pole-pair of stator-PMs, rotor-PMs, and windings are consistent with the theoretical analysis.

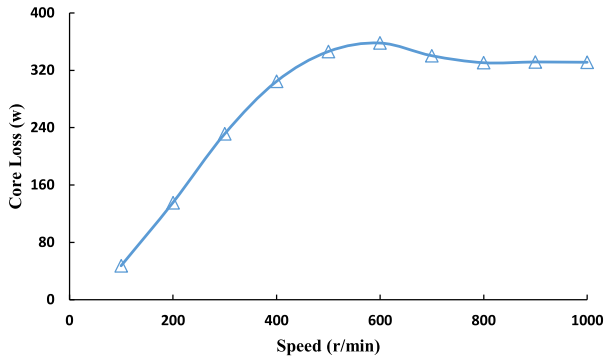


FIGURE 11. Measured core loss of the SSDPM machine.

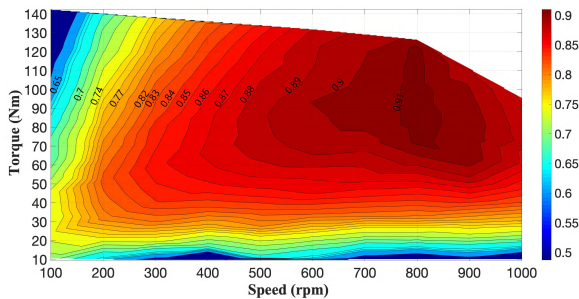


FIGURE 12. Efficiency map of the simulations.

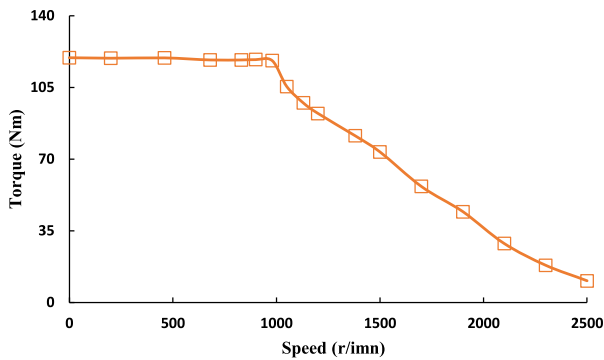


FIGURE 13. Torque-speed waveforms.

The core loss is an important limiting factor for constant power operation of the machine [24], [25]. Iron loss is generated by the stator and rotor. FEM is used to measure core loss of the machine at various speeds. The results are shown in Fig. 11.

The efficiency maps (Fig. 12) show that the maximum efficiency can reach up to 91%. This figure clearly demonstrates that the design principle is justified. The torque-speed characteristics of the SSDPM machine is shown in Fig. 13. This figure also shows that the rise in voltage that occurs as the speed increases when motor operates at rated speed. The constant torque stage ends once the voltage rises to the system’s limit. When the curve enters a flux-weakening control state, the speed of the motor will increase and it can reach a higher-than-rated speed. We note that the voltage of the machine remains steady by increasing the d axis current. The process is called a constant power stage. The SSDPM

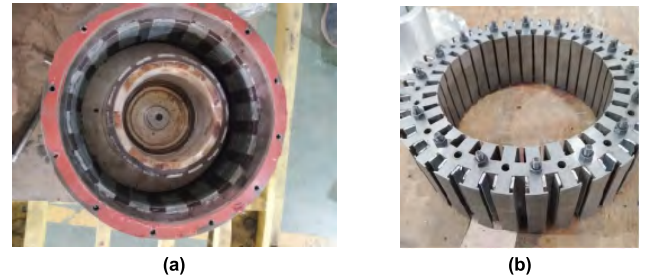


FIGURE 14. Structure of the proposed SSDPM. (a) Double rotor. (b) Double stator.



FIGURE 15. Test bench of the proposed SSDPM.

machine can keep constant power operation over a wide speed range.

#### IV. EXPERIMENTAL VERIFICATION

To illustrate the theoretical analysis and simulation results, the proposed machine is fabricated and shown in Fig. 14. The magnetic core of the inner and outer rotor is formed by lamination, which can effectively prevent energy losses from eddy currents [26]. To ensure mechanical strength of the mechanism, a fixed screw is placed on the iron core ring, between the inner and outer stator. A monolithic structure is made up of several stator rigid connections, stator supporting parts, motor shafts, coupling and rotating transformers. All components connect with the external fixed structure.

The test platform is shown in Fig. 15. The SSDPM motor is towed by the load motor. To convert the torque and speed signal into an analog or digital signal, the torque and rotational speed measure is used to relate the two motors. In this way, the power analyzer can calculate the mechanical power of the motor by receiving the data from torque and rotational speed measurer.

The no-load phase back EMF at 600 rpm is measured and compared to the FEM result in Fig. 16. The simulation produced a slightly higher voltage due to flux leakage around the shaft in experiments.

Fig. 17 and Fig. 18 shows the current response of the proposed machine when the speed of the rotor is 200 rpm.

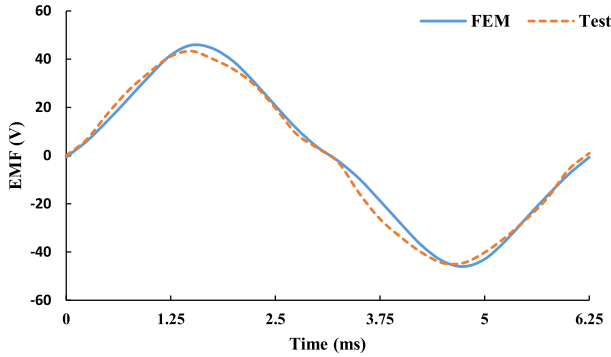


FIGURE 16. Back-EMF waveforms.

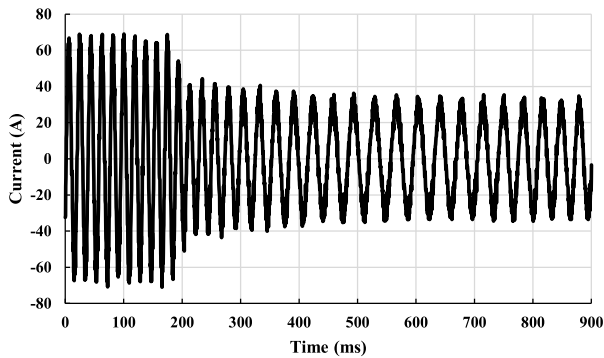


FIGURE 17. The current responses to reduce load.

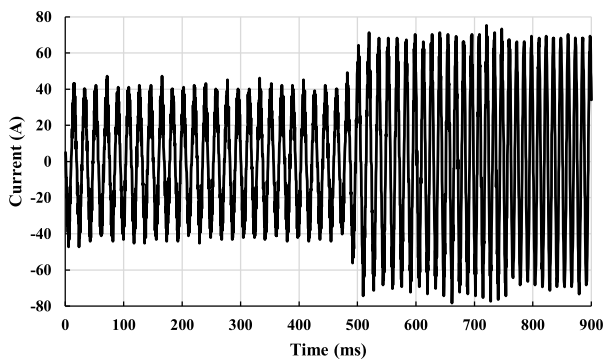


FIGURE 18. The current responses increase load.

The torque varies from 60 Nm to 30 Nm. In contrast, the torque is increased in the same way. Therefore, the machine can respond quickly when the load changes. The efficiency maps of the proposed machine can be achieved by drive experiment, as shown in Fig. 19. Meanwhile, the conditions and parameters between the FEM simulation and experiments should remain the same. To produce steady electromagnetic torque, the load inverter should make the SSDPM motor reach the specified speed. Moreover, the load machine output of maximum torque should be higher than the proposed machine. Compared with the proposed machine used for FEM analysis and the traditional PM machines, the experiments have lower efficiency. The reason behind this may be higher frequency and leakage resistance.

To verify the performance of the motors, vehicle tests are necessary. The drive system of an electric vehicle is shown

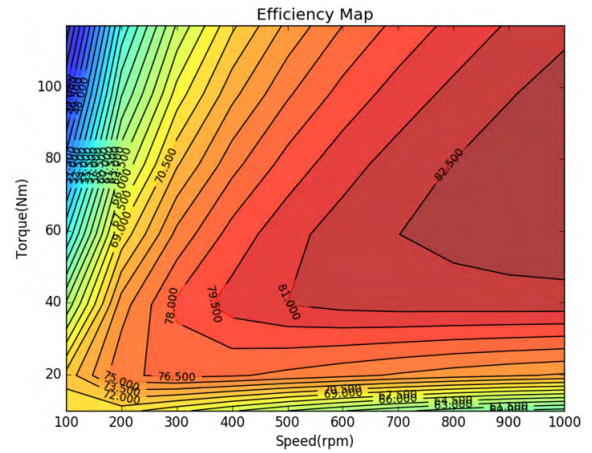


FIGURE 19. Efficiency map of the experiments.

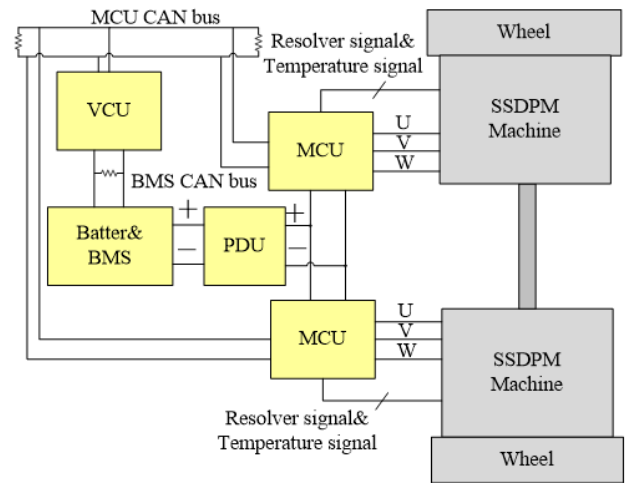


FIGURE 20. Drive system.

in Fig. 20. The vehicle driving system includes a power battery system, vehicle controller (VCU), microprogrammed control units (MCU), power distribution unit (PDU), two machines mounted on the wheels and any needed auxiliary equipment [27], [28]. Double MCUs are used to control the two machines respectively. The VCU relates to an MCU via a CAN bus. The VCU is related to the battery management system (BMS) via a BMS CAN bus, which is used to control the switching state of the main relay and the dc supply of the MCU. The VCU collects throttles, brakes and sends key signals to generate torque signals via logical operations. The torque signals transmitted by a CAN bus can be used to control torque via the MCU. Finally, the proposed dual-PM machine can achieve vehicle power control. Two machines are connected by a rear axle to form a rear bridge structure, as shown in Fig. 21. The frame diagram of the vehicle is shown in Fig. 22. To accelerate testing the performance of the proposed machine, the acceleration equation in the horizontal pavement can be characterized by

$$a = \frac{(T_{left} + T_{right})R - f}{m} \quad (6)$$



FIGURE 21. The rear axle of the wheel.



FIGURE 22. Test frame of the proposed SSDPM.

where  $m$  is the weight of the EV, which includes the test driver (approximately 550kg),  $f$  is the total resistance,  $R$  is the radius of each rear wheel (approximately 0.31725 m),  $T_{right}$  is the torque of the left machine and  $T_{left}$  is the torque of the right machine. For the test, the torque of both machines is 50 Nm.

If  $f$  is assumed to be zero, the theoretical maximum linear acceleration of the frame is about  $0.115 \text{ m/s}^2$ . Furthermore, the acceleration of the proposed machine should meet the linear relationship. Fig. 23 shows the torque and speed responses of acceleration. It takes about 22 seconds from 0 km/h to 10 km/h. The average acceleration of the experiment is  $0.11 \text{ m/s}^2$ . By comparing the experimental results with the results of the theoretical analysis, we find that the acceleration of the experiment is smaller than that

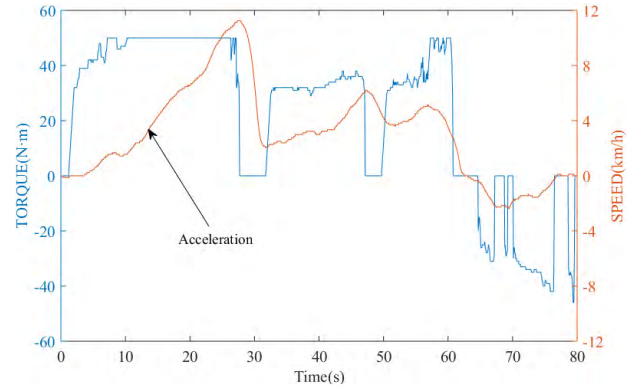


FIGURE 23. System torque and speed responses to the acceleration.

of the theoretical analysis. The reason is that in a real-world environment, total resistance cannot be neglected.

## V. CONCLUSION

In this paper, a novel synthetic slot Dual-PM machine is designed and analyzed, which employs two sets of PMs. Due to the dual PM excitation, the proposed SSDPM can achieve high torque density and a good flux modulating effect. The machine achieves effective coupling between the PMs and field coil excitations. The simulation and experimental results validate the effectiveness of this structure. By applying the FEM-GA coupled method, the optimal output torque can be achieved. Therefore, the proposed machine is suitable for low-speed high-torque applications.

## REFERENCES

- [1] Y. Chen, P. Pillay, and A. Khan, "PM wind generator topologies," *J. Elect. Electron. Eng.*, vol. 1, no. 1, pp. 125–129, 2008.
- [2] Y. Fan, K. T. Chau, and S. Niu, "Development of a new brushless doubly fed doubly salient machine for wind power generation," *IEEE Trans. Magn.*, vol. 42, no. 10, pp. 3455–3457, Oct. 2006.
- [3] S. Bayhan, H. Abu-Rub, and O. Ellabban, "Sensorless model predictive control scheme of wind-driven doubly fed induction generator in dc micro-grid," *IET Renew. Power Gener.*, vol. 10, no. 4, pp. 514–521, Apr. 2016.
- [4] Q. Wang and S. Niu, "Overview of flux-controllable machines: Electrically excited machines, hybrid excited machines and memory machines," *Renew. Sustain. Energy Rev.*, vol. 68, pp. 475–491, Feb. 2017.
- [5] M. R. Islam, A. M. Mahfuz-Ur-Rahman, M. M. Islam, Y. G. Guo, and J. G. Zhu, "Modular medium-voltage grid-connected converter with improved switching techniques for solar photovoltaic systems," *IEEE Trans. Ind. Electron.*, vol. 64, no. 11, pp. 8887–8896, Nov. 2017.
- [6] E. Gouda, S. Mezani, L. Baghli, and A. Rezzoug, "Comparative study between mechanical and magnetic planetary gears," *IEEE Trans. Magn.*, vol. 47, no. 2, pp. 439–450, Feb. 2011.
- [7] L. Cao, K. T. Chau, C. H. T. Lee, W. Li, and H. Fan, "Design and analysis of electromagnetic gears with variable gear ratios," *IEEE Trans. Magn.*, vol. 53, no. 11, Nov. 2017, Art. no. 8204706.
- [8] K. Atallah, S. D. Calverley, and D. Howe, "Design, analysis and realisation of a high-performance magnetic gear," *IEE Proc.-Electr. Power Appl.*, vol. 151, no. 2, pp. 135–143, Mar. 2004.
- [9] X. Zhang, "A novel coaxial magnetic gear and its integration with permanent-magnet brushless motor," *IEEE Trans. Magn.*, vol. 52, no. 7, Jul. 2016, Art. no. 8203304.
- [10] L. L. Wang, J. X. Shen, P. C. K. Luk, W. Z. Fei, C. F. Wang, and H. Hao, "Development of a magnetic-gear permanent-magnet brushless motor," *IEEE Trans. Magn.*, vol. 45, no. 10, pp. 4578–4581, Oct. 2009.
- [11] G. Liu, Y. Jiang, J. Ji, Q. Chen, and J. Yang, "Design and analysis of a new fault-tolerant magnetic-gear permanent-magnet motor," *IEEE Trans. Appl. Supercond.*, vol. 24, no. 3, Jun. 2014, Art. no. 0503205.

- [12] X. Guo, S. Wu, W. Fu, Y. Liu, Y. Wang, and P. Zeng, "Control of a dual-stator flux-modulated motor for electric vehicles," *Energies*, vol. 9, no. 7, p. 517, 2016.
- [13] Z. Chen, B. Wang, Z. Chen, and Y. Yan, "Comparison of flux regulation ability of the hybrid excitation doubly salient machines," *IEEE Trans. Ind. Electron.*, vol. 61, no. 7, pp. 3155–3166, Jul. 2014.
- [14] C. Liu and K. T. Chau, "Electromagnetic Design and Analysis of Double-Rotor Flux-Modulated Permanent-Magnet Machines," *Prog. Electromagn. Res.*, vol. 131, pp. 81–97, Sep. 2012.
- [15] J. Li, K. T. Chau, J. Z. Jiang, C. Liu, and W. Li, "A new efficient permanent-magnet Vernier machine for wind power generation," *IEEE Trans. Magn.*, vol. 46, no. 6, pp. 1475–1478, Jun. 2010.
- [16] Y. Liu, S. L. Ho, W. N. Fu, and X. Zhang, "Design optimization of a novel doubly fed dual-rotor flux-modulated machine for hybrid electric vehicles," *IEEE Trans. Magn.*, vol. 51, no. 3, Mar. 2015, Art. no. 8101604.
- [17] G. B. Hamadou, A. Masmoudi, I. Abdennadher, and A. Masmoudi, "Design of a single-stator dual-rotor permanent-magnet machine," *IEEE Trans. Magn.*, vol. 45, no. 1, pp. 127–132, Jan. 2009.
- [18] Y. Li, D. Bobba, and B. Sarlioglu, "Design and optimization of a novel dual-rotor hybrid PM machine for traction application," *IEEE Trans. Ind. Electron.*, vol. 65, no. 2, pp. 1762–1771, Feb. 2018.
- [19] S. L. Ho, S. Niu, and W. N. Fu, "A new dual-stator bidirectional-modulated PM machine and its optimization," *IEEE Trans. Magn.*, vol. 50, no. 11, Nov. 2014, Art. no. 8103404.
- [20] Y. Wang, W. N. Fu, and S. Niu, "A novel structure of dual-stator hybrid excitation synchronous motor," *IEEE Trans. Appl. Supercond.*, vol. 26, no. 4, Jun. 2016, Art. no. 0605805.
- [21] B. Chen and L. Li, "Semi-empirical model for precise analysis of copper losses in high-frequency transformers," *IEEE Access*, vol. 6, pp. 3655–3667, 2018.
- [22] L. Jian and K. T. Chau, "A coaxial magnetic gear with Halbach permanent-magnet arrays," *IEEE Trans. Energy Convers.*, vol. 25, no. 2, pp. 319–328, Jun. 2010.
- [23] Q. Wang, S. Niu, and L. Yang, "Design optimization and comparative study of novel dual-PM excited machines," *IEEE Trans. Ind. Electron.*, vol. 64, no. 12, pp. 9924–9933, Dec. 2017.
- [24] C. C. Mi, G. R. Slemon, and R. Bonert, "Minimization of iron losses of permanent magnet synchronous machines," *IEEE Trans. Energy Convers.*, vol. 20, no. 1, pp. 121–127, Mar. 2005.
- [25] V. Životić-Kukolj, W. L. Soong, and N. Ertugrul, "Iron loss reduction in an interior PM automotive alternator," *IEEE Trans. Ind. Appl.*, vol. 42, no. 6, pp. 1478–1486, Nov./Dec. 2006.
- [26] H.-Y. Kim and C.-W. Lee, "Analysis of eddy-current loss for design of small active magnetic bearings with solid core and rotor," *IEEE Trans. Magn.*, vol. 40, no. 5, pp. 3293–3301, Sep. 2004.
- [27] A. Emadi, Y. J. Lee, and K. Rajashekhara, "Power electronics and motor drives in electric, hybrid electric, and plug-in hybrid electric vehicles," *IEEE Trans. Ind. Electron.*, vol. 55, no. 6, pp. 2237–2245, Jun. 2008.
- [28] K. T. Chau, C. C. Chan, and C. Liu, "Overview of permanent-magnet brushless drives for electric and hybrid electric vehicles," *IEEE Trans. Ind. Electron.*, vol. 55, no. 6, pp. 2246–2257, Jun. 2008.



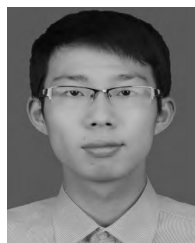
**QIUXUE WANG** was born in Heilongjiang, China. She received the B.E. degree in electrical engineering from the Lanzhou University of Technology, Lanzhou, China, in 2014. She is currently pursuing the M.S. degree in electrical engineering with Huaqiao University, China.

Her research interests include permanent magnet synchronous motor, new type of motor, and applied electromagnetics.



**RONGYAN SHANG** received the bachelor's degree from the Shenyang University of Technology, in 1999, and the master's and Ph.D. degrees from Hunan University, in 2006 and 2008, respectively.

From 1999 to 2003, she was an Assistant Engineer with Xiangtan electric manufacturing company. Since 2008, she has been with the College of Information Science and Engineering, Huaqiao University, China, where she is currently a Lecturer. Her research interests include motor and its control systems, dc transmission technology, power equipment on-line monitoring, protection, and fault diagnosis.



**FENYU CHEN** was born in Fujian, China. He received the B.E. degree in electrical and information engineering from Huaqiao University, Fujian, in 2016, and where he is currently pursuing the M.E. degree in electrical engineering.

His research interest includes vehicle dynamics and control for new energy vehicle.



**WEINONG FU** received the B.Eng. degree from the Hefei University of Technology, Hefei, China, in 1982, the M.Eng. degree from the Shanghai University of Technology, Shanghai, China, in 1989, and the Ph.D. degree from The Hong Kong Polytechnic University, Hong Kong, in 1999, all in electrical engineering.

He is currently a Professor with The Hong Kong Polytechnic University. Before joining the university in 2007, he was one of the key developers with Ansoft Corporation, Pittsburgh, PA, USA. He has about seven years of working experience with Ansoft, focusing on the development of the commercial software Maxwell. He has published 184 papers in refereed journals. His current research interests mainly include numerical methods of electromagnetic field computation, optimal design of electric devices based on numerical models, applied electromagnetics, and novel electric machines.



**WEI HUA** (M'03–SM'16) received the B.Sc. and Ph.D. degrees from the School of Electrical Engineering, Southeast University, Nanjing, China, in 2001 and 2007, respectively.

Since 2007, he has been with Southeast University, where he is currently a Professor with the School of Electrical Engineering. He has authored or co-authored over 140 technical papers. He is the holder of 30 patents in his areas of interest. His teaching and research interests include the design, analysis, and control of electrical machines.



**XINHUA GUO** was born in Fujian, China. He received the degree from the Nanjing Institute of Technology, in 2000, the master's degree in agricultural electrification and automation from Jiangsu University, Jiangsu, China, in 2006, and the Ph.D. degree in electrical engineering from The Institute of Electrical Engineering (IEE), Chinese Academy of Sciences (CAS), Beijing, in 2010.

He was a Research Assistant with IEE, CAS. And he had been with TDK, from 2000 to 2004. He is currently an Associate Professor with Huaqiao University, and also with the Fujian Engineering Research Center of Motor Control and System Optimal Schedule, Xiamen, China. His current research interests include IGBT packaging technology, PMSM and its drive control for EV, and special motor and its drive control, such as double mechanical port motor and wheel hub motor.